Massachusetts Institute of Technology,
École Normale Supérieure

Geometrically induced rigidity of thin shells & Negative Poisson's ratio structures

First year Master's Degree research internship

Claude Perdigou
claude.perdigou@ens.fr

Under the supervision of
Pr. Pedro Reis

February, 8th - July, 31st 2010

Abstract

This report presents new experimental and theoretical results on the mechanics of thin shells. In the first part we will focus on thin shells of revolution and geometrically induced rigidity. The theory of spherical thin shells will be extended to axisymmetric ellipsoids. Experiments explore the linear and nonlinear regime for plate and point load on thin shells of revolution. In the linear regime we compare the effective Young's modulus with theoretical predictions. In the nonlinear regime, we will study buckling and stress localization.

The second part of this report features recent advancements in the creation of a simple three dimensional structure showing a negative Poisson's ratio. Although the structure created does not show an auxetic behavior under uniaxial compression, we bring to light a mechanical instability that occurs when uniform pressure is applied.

Keywords : mechanics of thin structures, geometrically induced rigidity, theory of thin shells, stress localization, mechanical instability, negative Poisson's ratio.

Résumé

Ce rapport de stage présente des résultats nouveaux en mécanique des structures fines. La première partie se concentre sur les coquilles fines de révolution, et en particulier sur l'influence de la géométrie sur les propriétés mécaniques de ces objets. Des résultats expérimentaux et théoriques sont présentés. D'un point de vue théorique, on étend une théorie déjà existante pour les coquilles sphériques au cas des coquilles ellipsoïdes. Expérimentalement, on compare le régime linéaire aux prédictions théoriques, et on étudie le régime non linéaire ; en particulier le cas du flambage et de la localisation de la contrainte.

La seconde partie de ce texte expose des progrès récents dans la création d'une structure tri-dimensionnelle présentant un nombre de Poisson négatif. Bien que la structure obtenue ne présente pas ce comportement lors d'une compression axiale, on met en évidence une instabilité mécanique lorsqu'une pression est appliquée uniformément.

Mots-clés : mécanique des structures fines, influence de la géométrie sur les propriétés mécaniques, théorie des coquilles fines, localisation de la contrainte, instabilité mécanique, nombre de Poisson négatif.

Contents

Introduction

My internship took place at the Massachusetts Institute of Technology in Cambridge, USA. From early February to the end of July, I worked with Professor Pedro Reis in the departments of Mechanical Engineering and Civil and Environmental Engineering. I also had the opportunity to work with Professor Katia Bertoldi from the School of Engineering and Applied Science of Harvard University, also in Cambridge.

During my internship I worked in the EGSLab (Elasticity, Geometry and Statistics Laboratory) and the most important results I obtained while experimenting on thin shells are detailed in the first part of this report. My work is concerned with the mechanical properties of thin shells, in the linear and nonlinear regimes. I studied both the experimental and theoretical aspects, all of which are reviewed in this first chapter. Some important experimental technicalities and secondary results I studied during my internship can be found in appendix.

The second chapter of this report is dedicated to a secondary project that started as soon as I arrived. A joint project between my advisor Pedro Reis and his friend Katia Bertoldi regarding structures with a negative Poisson ratio was already on the agenda at the time of my arrival. Seeing my interest in the project, they offered me to take part in it. The main idea was to create a three dimensional structure showing a negative Poisson ratio. This technical notion, along with the results obtained while working on this project are detailed in the second chapter of this report.

Most of the work I have done is on the mechanics of thin shells, but my secondary project took more and more importance towards the end of my internship. For that reason, an important part of my report is dedicated to it.

Chapter 1

Geometrically induced rigidity of thin shells

1.1 An egg affair

Thin shells are a key element in various domains, such as architecture, biology and even sports. The most common example of geometrically induced rigidity is to be found, very simply, in an egg. When compressed along their longest axis, eggshells are very hard to break, but compressed along their smaller axis, eggs are much more fragile. Eggs inherit their surprising rigidity mainly from structural properties ; but this anisotropy is only due to geometry.

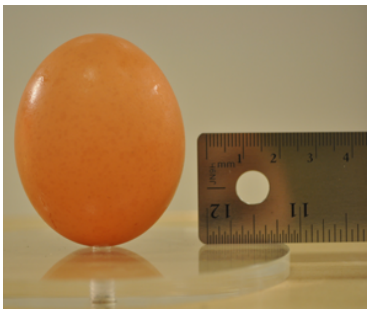

(a) The egg used for this experiment

Figure 1.1: How to make an omelette.

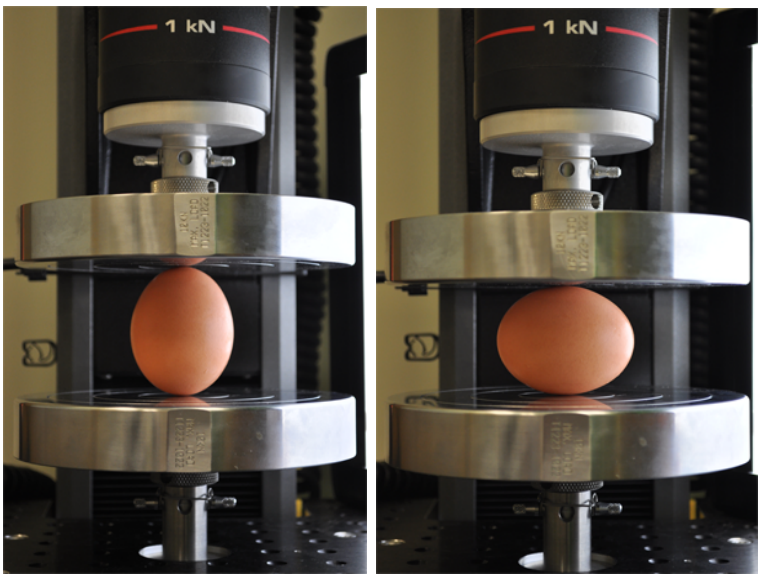

(b) Long axis compression (c) Small axis compression

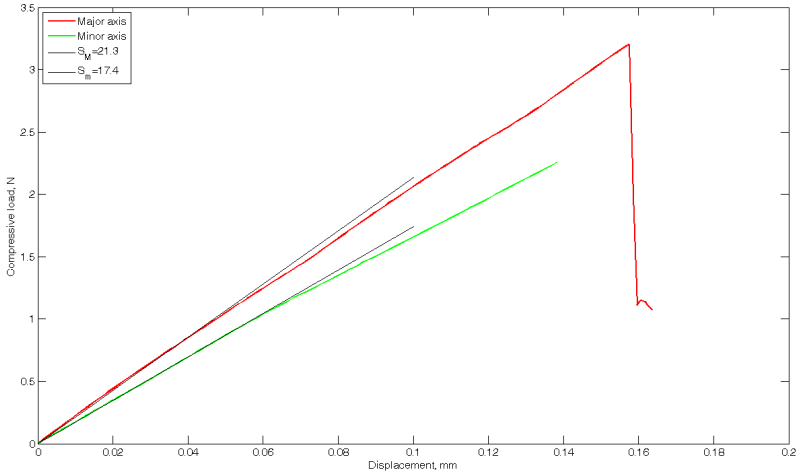

(d) Long and Small axis Load Displacement curves

Figure 1.1: How to make an omelette.

This major difference between the two directions of compression is obvious, and we would like to understand how the geometry influences mechanical properties.

Another domain of interest in thin shells is their nonlinear behavior at large deformation, the study of this domain was also one of the aims of my internship.

Simulations have been done by Ashkan Vaziri at Northeastern University for the case of spherical shells [1].

1.2 The birth of a shell

Upon my arrival at the MIT, the lab I was to work was not ready yet, so that I had time to work on theoretical and computer-related problems. Of course, I helped to set up the lab, but even before that, my very first task was to install the various software that might be needed for future work.

Regarding the creation of our shells, many options seemed possible. We could either print them directly with a 3D printer, order them online from a specialized company, or cast them in molds that had to be created.

All these methods implied one thing : having a .STL file (basic exchange format for 3D designs).

For that reason, the first weeks of my internship were busy with various software tasks, which included learning how to use Solidworks. Once I had acquired enough practice and skill with Solidworks, I was able to produce the design of our first shells, along with another design for the mold.

1.2.1 Option 1 : 3D printing

An extensive description of the 3D printer is provided in appendix C, but the important conclusion to be drawn, is that the shells we made with the printer were very fragile. Moreover some defects were present and the material was already torn in several places. Last, the soft material used for printing has important visco elastic properties that make it unfit for dynamic experiments : it takes minutes for the shells to recover from a compression test, and hours for them to really and completely relax all internal stresses.

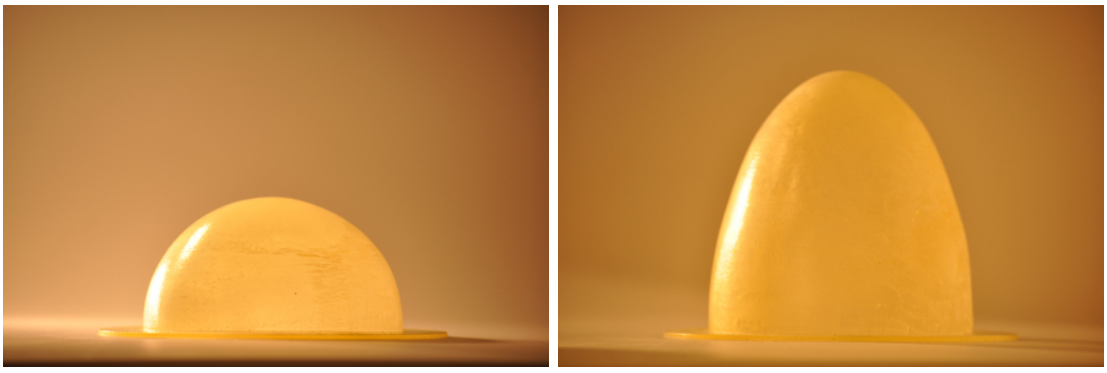

(a) Spherical Shell (b) Ellipsoidal Shell

Figure 1.2: 3D Printed Shells.

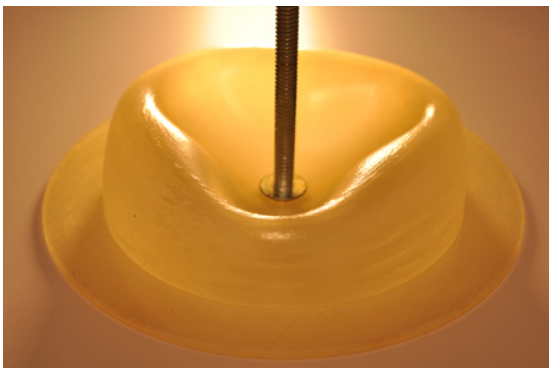

(c) Spherical Shell under point load

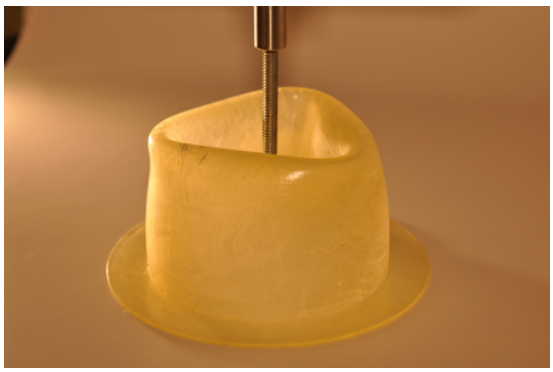

(d) Ellipsoidal Shell under point load

Figure 1.2: 3D Printed Shells.

Still, it was useful to have these shells, we used them when studying the linear regime, cf part 1.4.1. Moreover their big size and transparency made them appropriate for imaging purposes.

1.2.2 Option 2 : Casting

We then tried a slightly different approach : we decided to 3D print the mold for our shells and then to cast them, using a self-curing polymer. This polymer is used by dentists to cast teeth molds, and only requires two components to be mixed in equal quantities.

Figure 1.3: Full span of polymers available for casting.

I could use four different polymers, each of a different Young modulus and color. I measured the Young's modulus of these four kinds of polymers and the results can be

found in appendix A.

To print the molds I used another printer, available as a service in one of the mechanical shops of the MIT. It prints hard plastic (ABS), which is appropriate for a mold ; one of our typical jobs takes approximately 30 hours. The complete process can be summarized with these three pictures :

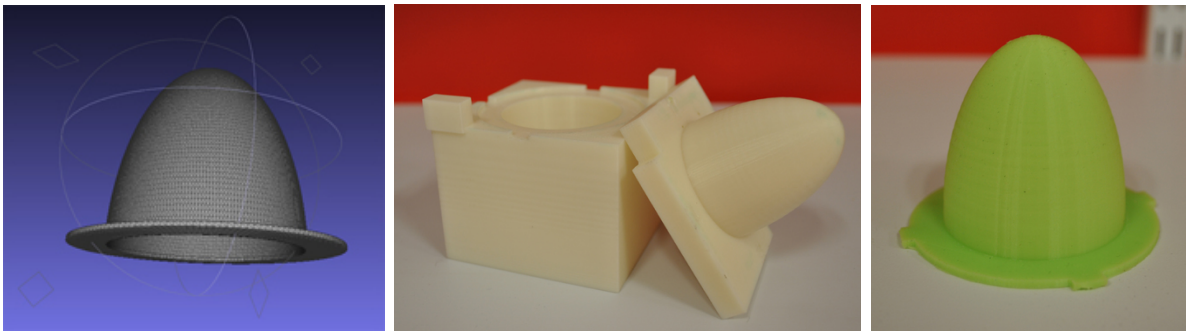

(a) CAD Model (b) Printed Mold (c) Cast Shell

Figure 1.4: From the virtual to the rubber shell.

1.2.3 First experiment

The first device I used for my experiment was made of a linear stage driven by a stepper motor ; it was operated through labview so that I could control the displacement speed. A force sensor was connected to this linear stage and it was possible to choose between plate and point load by putting either a screw or a plastic plate at the tip of the sensor.

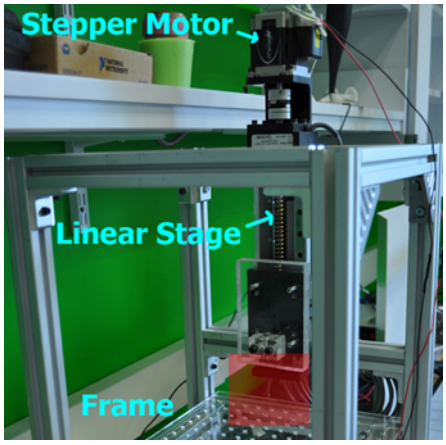

Figure 1.5: Custom built Instron type machine. The red zone is where the force sensor used to be.

I first tested the printed shell in the linear regime, and the curves I obtained are the following :

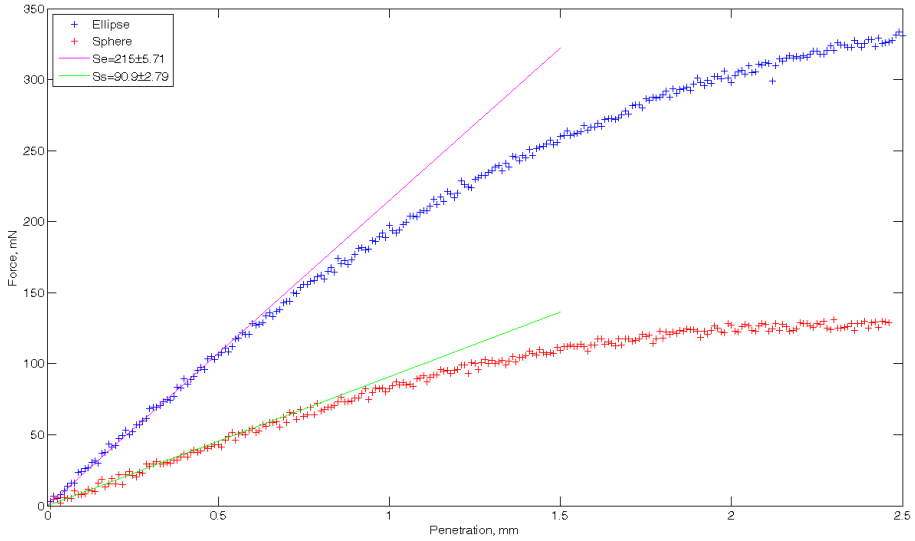

Figure 1.6: Linear regime and plateau for the printed shells.

There is a very clear difference between the response of the ellipsoid and that of the sphere. The slope of the linear part is roughly twice as important for the ellipsoid as for the sphere. It is a very interesting feature, which deserves to be understood theoretically. I dived into the theory of thin shells during the first months of my internship, and what I found is detailed in the next section.

1.3 Theory of thin shells

The shape of a thin shell has a sensible influence on its mechanical properties, e.g. on the Young's modulus that can be measured. In this section we will extend the theory of thin shells for spherical shells to shells of revolution of any shape. We will focus particularly on axisymmetric ellipsoids.

1.3.1 Shells of revolution, main equations

First, we are going to define the conventions and obtain general equations for thin shells of revolution.

The following notations were used for the derivations I made :

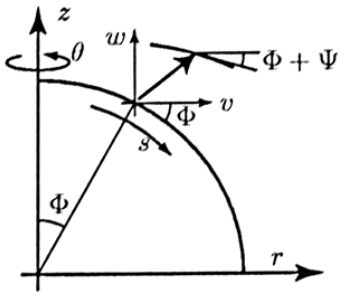

With

$$\frac{dr}{ds} = r' = cos\Phi$$

$$\frac{dz}{ds} = z' = -sin\Phi$$

Let me recall here the principal results obtained by B. Audoly and Y. Pomeau in their book *Elasticity and Geometry : From hair curls to the nonlinear response of shells*[2]. For further detail on the following derivations, please refer to this book.

The shells being shells of revolution, the problem is axisymmetric and $\epsilon_{s\theta}$ vanishes. Hence we will more simply use ϵ_s and ϵ_θ to denote the components ϵ_{ss} and $\epsilon_{\theta\theta}$ respectively. If we compare two formulations of a length element, the following expressions appear :

$$\epsilon_s = r'v' + z'w' + \frac{1}{2}(v'^2 + w'^2)$$

$$\epsilon_\theta = \frac{v}{r} + \frac{v^2}{2r^2}$$

When we introduce $\Psi = z'v' - r'w'$, which is the change of orientation of the tangent after deformation, the strain component ϵ_s becomes $\epsilon_s = r'v' + z'w' + \frac{1}{2}\Psi^2$, after neglecting a term of second order. This first order approximation also lets us write $\epsilon_\theta = \frac{v}{r}$.

Since we use Hookean elasticity and considering an axisymmetric problem, the stress-strain relations for the thin shells are :

$$\sigma_s - \nu\sigma_\theta = E\epsilon_s$$

$$\sigma_\theta - \nu\sigma_s = E\epsilon_\theta$$

Using the balance of force and minimising the energy, one can obtain the following equilibrium equations [2] :

$$h(\sigma_\theta - \frac{d}{ds}(r\sigma_s[cos\Phi - \Psi sin\Phi])) = rf_r$$

$$h(\frac{d}{ds}(r\sigma_s[sin\Phi + \Psi cos\Phi] + \frac{D}{h}[(r\Delta w)' - \Delta w])) = rf_z$$

Where $D = \frac{Eh^3}{12(1-\nu^2)}$ and w is the displacement along the vertical axis.

1.3.2 Ellipsoids of revolution

The equations obtained previously are valid for shells of revolution of any shape. From now on, we shall concentrate on shells of ellipsoidal shape.

The shape of the shell is as follows :

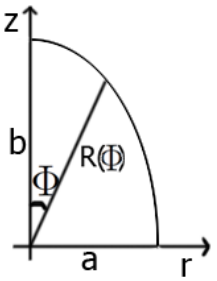

Figure 1.7: Notations used to describe the shell.

Here one can derive the distance

$$R(\Phi) = \frac{ab}{\sqrt{a^2cos^2\Phi + b^2sin^2\Phi}}$$

And then writing $ds = R(\Phi)\ d\Phi$ and using $dr = ds\ cos\Phi$ we obtain

$$r = \frac{ab}{\sqrt{b^2 - a^2}}\ sinh^{-1}(\frac{\sqrt{b^2 - a^2}\ sin(\Phi)}{a})$$

If $\Phi << 1$ then $r \approx s$ and

$$s = \frac{ab}{\sqrt{b^2 - a^2}}\ sinh^{-1}(\frac{\sqrt{b^2 - a^2}\ \Phi}{a})$$

We notice that if $a = b = R$ we get the right relation for a spherical shell.

We assume a frictionless contact under plane load conditions, if we neglect terms of second order in Φ and Ψ, the equations of mechanical equilibrium become :

$$h(\sigma_\theta - \frac{d}{ds}(s\sigma_s)) = 0$$

$$h(\frac{d}{ds}(s\sigma_s[\Phi + \Psi])) + D\frac{d}{ds}((s\Psi')' - \frac{\Psi}{s}) = rf_z$$

Thus we find that $\sigma_\theta = (s\sigma_s)'$, and using the equations above to eliminate σ_θ one can obtain the dimensionless equation :

$$s^2\sigma_s'' + 3s\sigma_s' + \Phi\Psi + 1/2\Psi^2 = 0$$

If we consider a disc-like contact under a plane load, the following relation is always true on the contact zone $\Psi + \Phi = 0$, i.e. the contact zone is flat. Hence the equation above becomes :

$$s^2\sigma_s'' + 3s\sigma_s' - 1/2\Phi^2 = 0$$

We then define $\delta = \sqrt{b^2 - a^2}$ and $R = \sqrt{ab}$ to write $\Phi = \frac{a}{\delta} sinh(\frac{s\delta}{R})$.

This leads to the final differential equation we have to solve to know the stress in the disc-like contact region with a plane load :

$$s^2\sigma_s'' + 3s\sigma_s' = \frac{a^2}{2\delta^2} sinh^2(\frac{s\delta}{R})$$

In the approximation of small deformations where $s/R << 1$, this equation becomes

$$s^2\sigma_s'' + 3s\sigma_s' = \frac{a}{b}\frac{s^2}{2}$$

By integration of this equation we obtain

$$\sigma_{s,ellipsoid} = \frac{a}{b}\sigma_{s,sphere} \propto \frac{a}{b}\frac{s^2}{16}$$

Thus the only difference with a spherical shell of revolution is a factor a/b for the radial stress $\sigma_{s,sphere} \propto \frac{s^2}{16}$.
Using the stress-strain relation

$$\sigma_{s,ellipsoid} - \nu(s\sigma_{s,ellipsoid})' = \frac{a}{b}[\sigma_{s,sphere} - \nu(s\sigma_{s,sphere})'] = E\epsilon_s$$

we clearly see that the ellipsoid problem is the same as the spherical one, provided we consider an effective Young's modulus $E_{eff} = \frac{b}{a}E$ for the ellipsoid.

This very simple theoretical result means that a shell twice as high as a spherical shell should be twice as stiff. We will verify it experimentally, by testing the mechanical response of various shell geometries in the linear regime.

1.4 Experiments

Geometrically induced rigidity of shells can be probed easily by doing compression tests. Two domains can be studied, the linear regime, and the nonlinear one, in which a localization of the stress is to be seen. In the experiments described throughout this section I made extensive use of a laser cutter, (for more details on this exceptional tool,

please see appendix D).

Systematic experiments could begin when my home made force sensor was replaced by a commercial Instron. With the Instron's load cell new limit of 10 N, I could explore the whole behavior of the shells, without having to see the sensor saturate after the first few millimeters. We actually found the Instron impossible to use because its generic loading system was too heavy for our very sensitive load cell. Therefore we had to devise another loading system.

We had to pay attention to the fact that the pressure inside the shells must not build up, which means that its support must have holes. One is confronted with the same problem when running a plate load experiment, the loading plate must have holes to release the pressure from the cavity formed in the cap of the shell. Moreover, we required to be able to take some photographs, which means that we had to rethink completely the experimental set-up. We eventually came up with a reversed set-up :

Figure 1.8: The final Instron set-up that enables imaging.

In this set-up, the shell is clamped under the force sensor, and moves with it towards a fixed obstacle : either a screw or a plate. This plate is transparent and was cut to the right dimensions with a laser cutter. Thus it is possible to fix a camera under the whole set-up, and the camera will see through the plate. Using a circular neon fitting under the shell to provide some light, I could get very fine pictures, with a good contrast, to study the nonlinear regime.

1.4.1 Linear Regime

By experimenting on the linear regime we can measure the stiffness of a structure, i.e. its effective Young's modulus. We have just seen that the effective Young's modulus measured should grow linearly with the ratio b/a, where b and a are respectively the large and the small radii of the ellipsoid of revolution. (cf section 1.3)

The theory of thin shells assumes a frictionless plate load. Practically, it is not easy to get a frictionless contact with a plate, so we might prefer a point load requiring the use of a screw. Moreover, the linear regime implies deformations that are so small that we do not see any cap inversion, so that the deformed zone remains very flat. This explains why, experimentally, the curves for linear regime are very similar for point and plate loads.

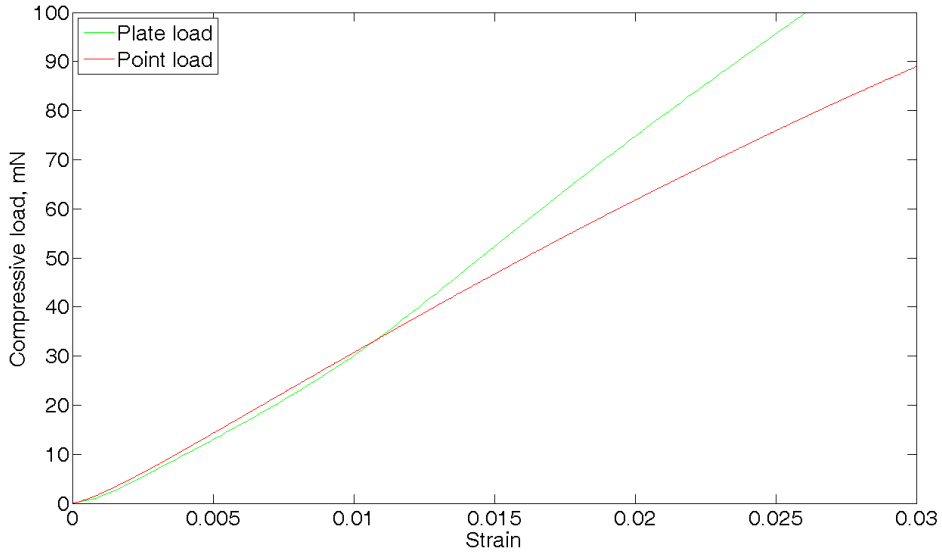

Figure 1.9: The linear regime is roughly the same for point and plate loads.

We expect shells of different geometry to have different effective Young's moduli. I tested four different materials of different bulk Young's modulus, and different thicknesses of shells.

With the right normalization, we would like our data to collapse to a few curves, different only if the geometry of the shell changes. To normalize the force, we use the quantity $Y * h^2$, to normalize the displacement, the quantity $R = \frac{a^2}{b}$. Here are the curves obtained :

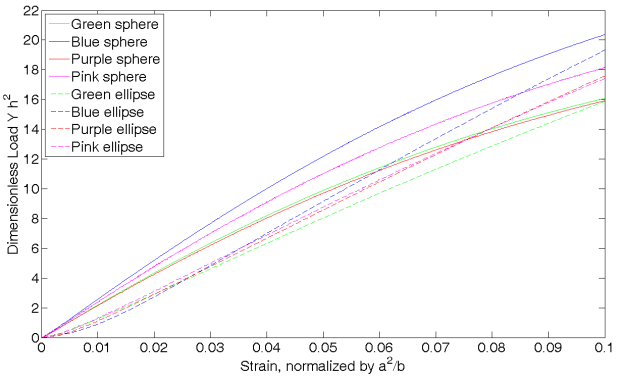

(a) 2 mm thickness

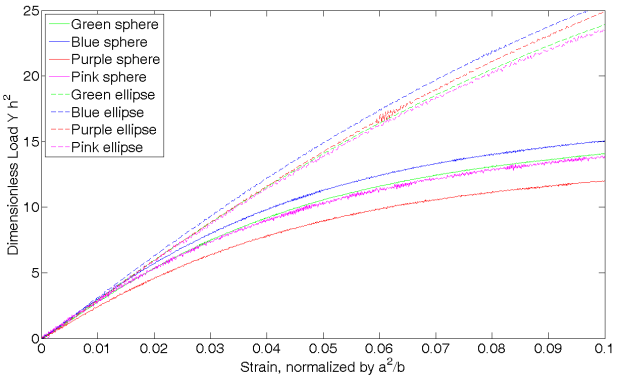

(b) 1 mm thickness

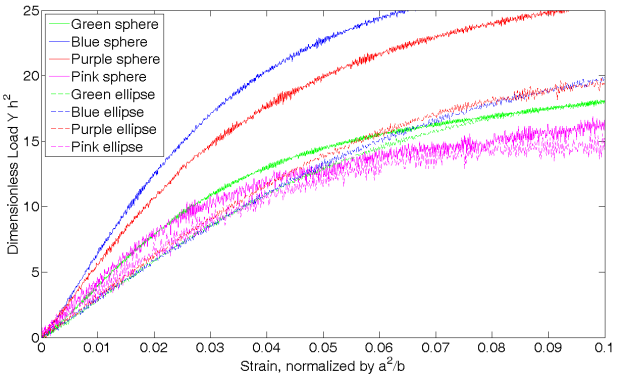

(c) .5 mm thickness

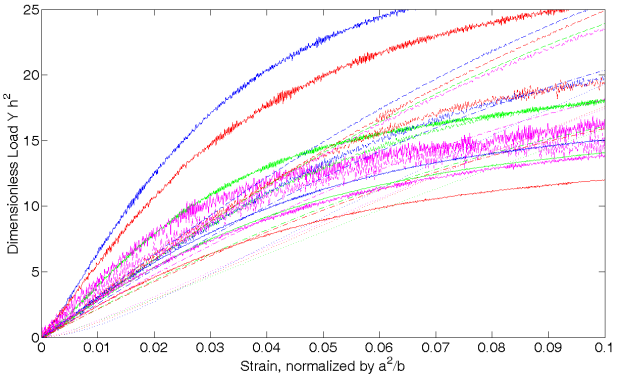

(d) All thicknesses

Figure 1.10: Stress strain curves for shells of different thicknesses. Spheres, $\frac{b}{a} = 1$; Ellipses, $\frac{b}{a} = 2$

This normalization works well, because it takes into account the difference in geometry when normalizing the strain, and the difference in thickness when normalizing the force.

By fitting the linear regime of the compression tests, I can get an effective Young's modulus and compare it for shells of different shapes but similar thickness.

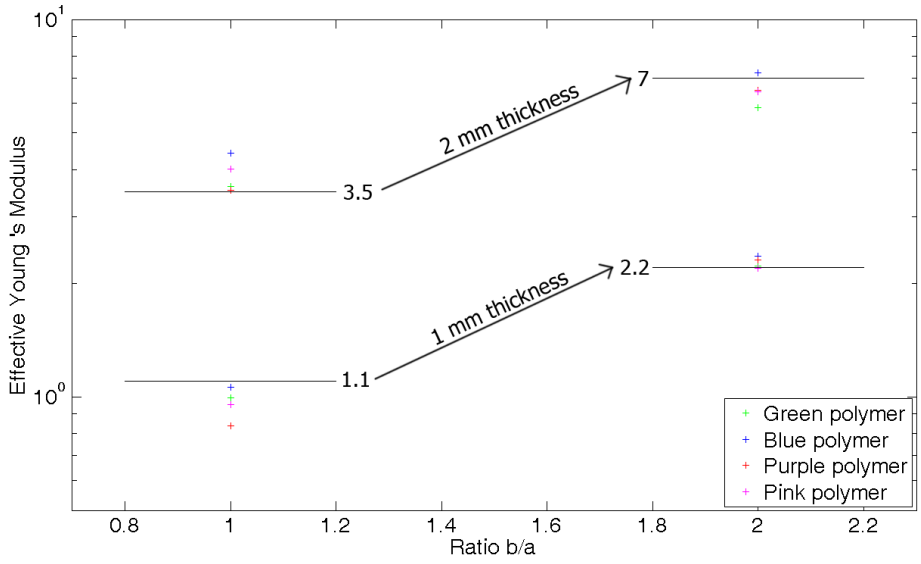

Figure 1.11: Young's modulus compared to geometrical ratio $\frac{b}{a}$

This last image does not show the results for the .5 mm shells. Although those shells should have the best behavior, they become too soft, even for the precise load cell I use. Hence, the measurements bear a lot of noise and the results are hard to interpret. Another problem is the uncertainty about the thickness. Such uncertainty, although not a problem for thicker shells, starts to be a real issue for the thinnest ones. Please see appendix B for more details.

1.4.2 Nonlinear regime

The nonlinear regime of compression of the shells is a very rich and interesting subfield of experimentation, mainly because it evidences a strong cleavage between the shells response to point load and plate load.

Point load, localization of the stress

Under point load, the behavior observed is first a progressive inversion of the cap of the shell, but after $\approx 80\%$ strain, the stress localizes into ridges forming geometrical figures (e.g. triangles).

This behavior has nothing to do with the material used : it depends only on geometrical properties. For example, a shell twice as big and thick as another one, will have the same localization patterns.

This experiment was done on the 1 mm thick ellipsoid shells ($\frac{b}{a} = 2, a = 25\ mm$), and I compared the four different materials I dipsosed of. Using a very low strain-rate, photographs were taken every 10 seconds, which allows us to track the position of the ridges. Superposition of the result leads to this graph :

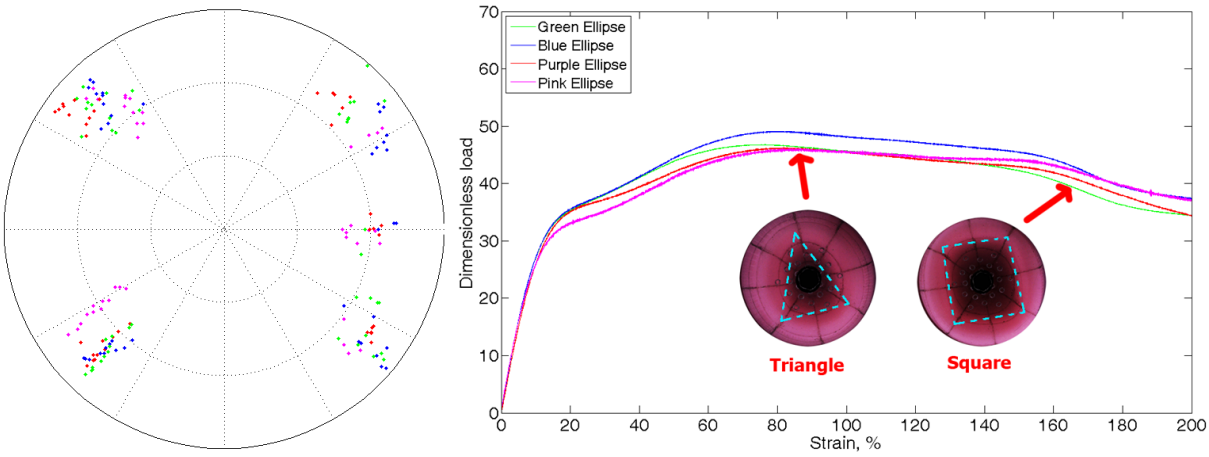

(a) Position of the ridges

(b) Typical stress strain curve obtained.

Figure 1.12: Position of the ridges under large deformation point load. 1 mm thick shells.

The farther from the center the points are, the larger the deformation is. First, we see that all shells show the same behavior ; localization into a triangular shape, and then into a square. The transition between the triangle and the square pattern is very hard to track, but a new ridge seems to appear between two others, the other ridges then migrate a little to form a square.

This localization pattern depends only on the size and on the thickness of the shell. The only other shells thin enough to show localization I had were the .5 mm, on which I ran the same experiment. They have exactly the same pattern : they form a triangle, then a square.

Plate load, buckling

Under plate load, the shells do not invert their cap, but buckle instead. The buckling occurs on the middle of the shell and looks like this :

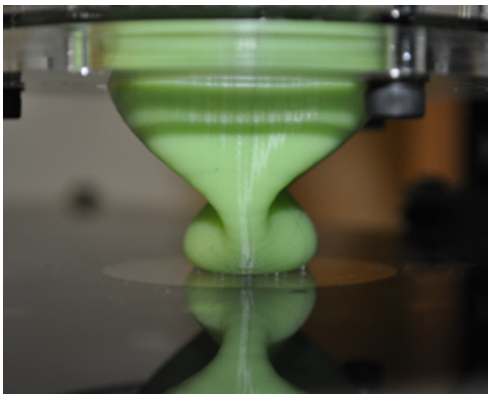

Figure 1.13: The buckling mode when plate load is used.

The buckling creates two depressions on two opposite sides of the shell, which is accompanied by an important release of the stress. The buckling is rate dependant, when the loading is slow enough, the buckling appears first on one side, and a little later on the other side. The same stress is released in the end, but in two steps.

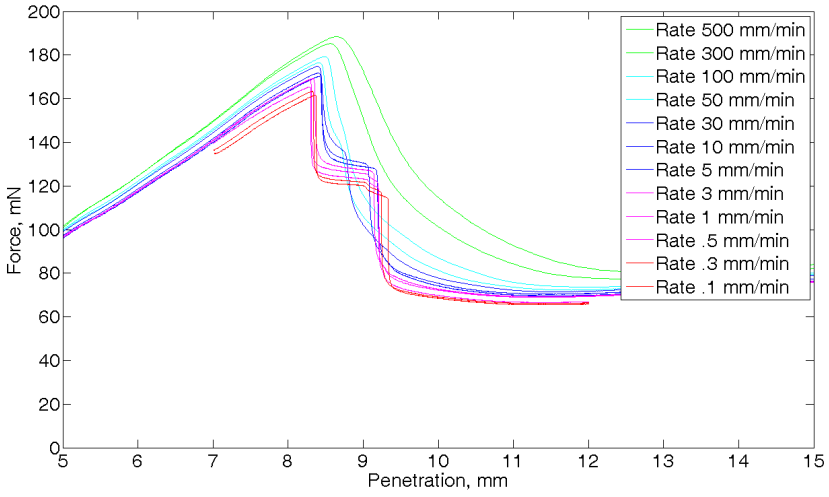

Figure 1.14: The buckling occurs in different ways depending on the strain rate.

In fact, the behavior of the shells in this regime is more than just rate-dependant. Sometimes we see a cap inversion before the buckling occurs, and sometimes the surface remains flat.

In the case of the spherical shells, we do not see buckling happening : just a cap invertion after a certain strain. When the load is slowly removed the phenomenon shows a hysteresis. Unfortunately I had to leave the study of these very interesting behaviors

for later work.

Experimentally looking at the linear and non-linear behaviors of thin shells is a very rich but also very wide field of research. During my experiments, many side questions arose, such as : What is the ridge height during the compression ? Do the curves I study depend on the position of the screw ? Does the material used have aging issues ? Is the uncertainty about the thickness implied by the casting process a real issue ? Is the 3D printing process precise enough to guarantee a precise thickness ? Answers to these questions can be found in the appendix B : additional work.

The following part of my report describes the side project I have also been working on during my internship.

Chapter 2

Negative Poisson's ratio structures

The Poisson ratio of a structure measures how much it expands in other directions when compressed along one axis. An incompressible material has a Poisson ratio of 1/2, since when you compress it in one direction, it expands in the two other directions while keeping the same volume. A sponge would have a Poisson ratio of 0, because when you compress it, it doesn't expand : you merely poke a hole in it and the sides do not swell. The Poisson ratio has an upper boundary of 1/2, and its lower boundary is not 0, but -1. Some structures, when compressed in one direction will also shrink in the other two. Note that a structure that swells in two directions when pulled in the third also has a negative Poisson ratio. These structures are often very complicated and reentrant. Materials with this property can also be called auxetics.

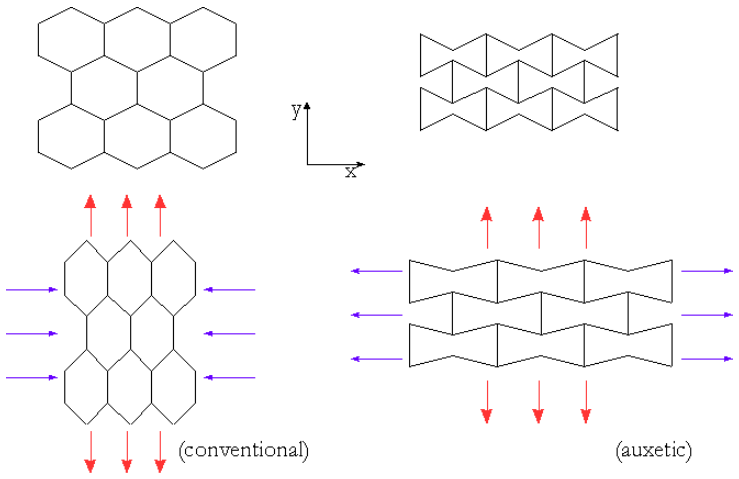

Figure 2.1: An example of a self-penetrating structure with a negative Poisson ratio.

In the past, one of the domains of interest of my advisor was to create a simpler structure displaying this property.

2.1 2D structure

In a work done by K. Bertoldi, T. Mullin and P. Reis [3] in Manchester, they designed a simple 2D structure with a negative Poisson's ratio.

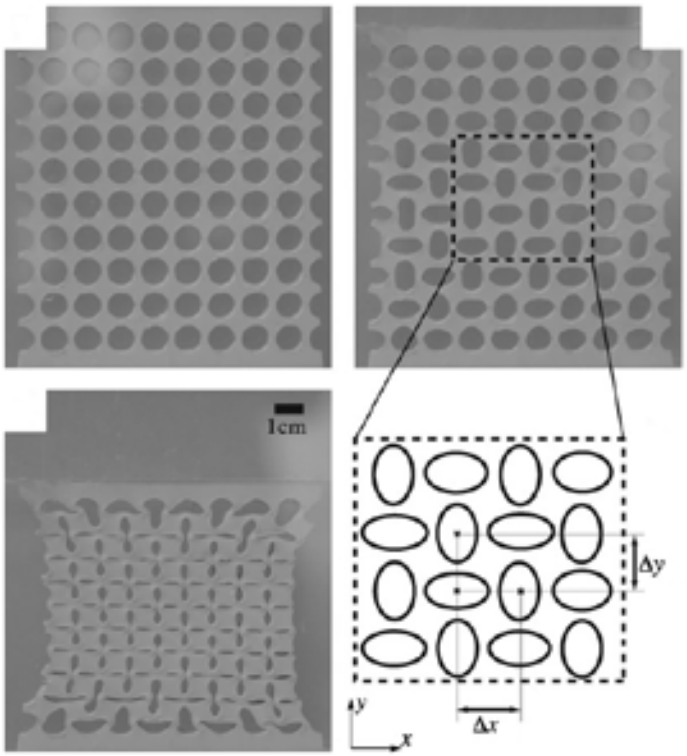

Figure 2.2: 2D structure showing a negative Poisson's ratio.

As shown on the image above, the array of holes on the structure deforms in a 4*4 regular pattern of ellipses. This is what makes a negative Poisson's ratio possible : the knots of the lattice rotate in opposite directions, without frustration, and the whole structure collapses.
I was very excited by this project, and my advisor offered me to take part in it with Professor Bertoldi in Harvard. The objective was to create a structure of the same simplicity, with the same amazing property, but in 3D.

2.2 Unfolding the third dimension

The first idea, that came naturally to mind, was to create the same object by repeating the pattern along the third direction of space to make an object that looks like this :

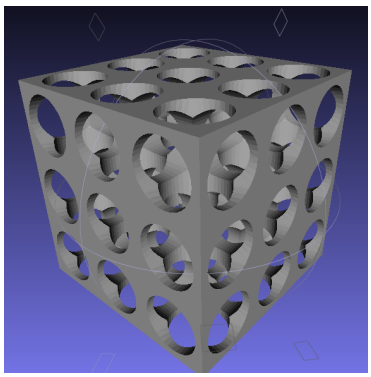

Figure 2.3: A simple 3D structure based on the previous 2D structure.

The unit cell is a cube pierced of three cylindrical holes. Another unit cell we tried, was made by scooping a sphere out of cube. Professor Katia Bertoldi in Harvard and her postdoc Jongmin Shim are running ABAQUS simulations on this project, and they found that the first compressive mode for these structures is exactly the same as for the 2D structure. It means that the structure shrinks only in one of the two directions orthogonal to the load. In the other direction, the side of the cube remains flat.

A second compressive mode triggered our attention, but was not further studied because the project took a new direction soon after.

On a trip to New York I found in a gift shop a very simple toy made of plastic that has this shape :

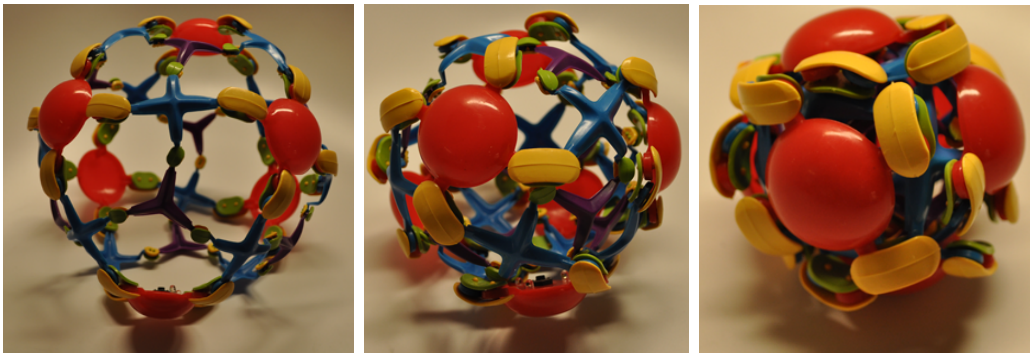

(a) The toy completely unfolded (b) The toy being folded (c) The toy completely folded

Figure 2.4: An auxetic toy ?

When compressed, this toy shrinks to form a smaller ball, its edges rotating, thanks to hinges, in a very peculiar manner. This toy was exactly what we were desperately trying to create. To get a 3D structure from the 2D one, we did not need to repeat the pattern in the third dimension, we just had to fold it into a sphere !

2.3 A spherical trap

Thus, we found ourselves with a very nice optimization problem on our hands : how to put 24 holes on a sphere ? I did not solve it analytically, but chose to design it directly with Solidworks. Here is the model I came up with :

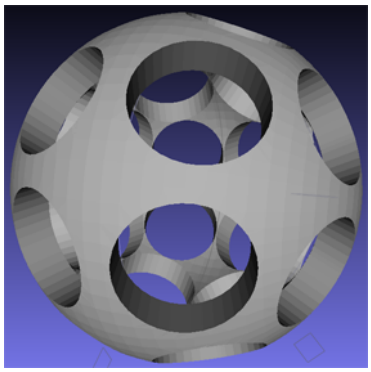

Figure 2.5: The CAD model of the toy.

Then simulations were run by Jongmin with various thicknesses and various hole sizes. If one uses a plate load, nothing specific happens, and the ball just buckles after a while. But if an isotropic pressure is applied on the exterior, the ball does fold neatly in this shape :

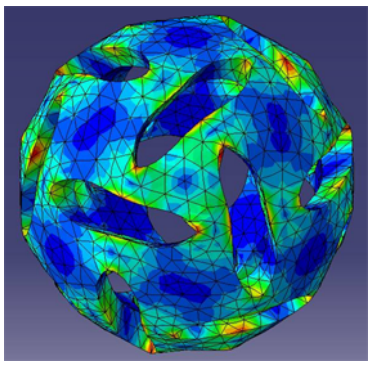

Figure 2.6: Simulated behavior under homogeneous pressure on the outer surface.

This was a very exciting result. The ball does not really have a negative Poisson ratio, since the shape cannot be obtained by compression ; but it makes a very neat cage. This is a mechanical instability, and the material of the sphere is elastic, so that the ball can repeat the same behavior : unloading it will reopen the cage, and it will be possible to close it again, etc...

To build such a struture experimentally, we considered the various simulations, which helped us to settle on one specific design. Unsurprisingly, the folding happens for

thicker shells (that will not buckle out of plane before) and bigger holes (more void makes the edges thinner and easier to bend).

Now used to the casting methods, I designed and printed a mold for this new object. Each hole has a small membrane so that it is possible to suck air out of the final model, and by glueing two halves with some polymer, I could get the first ball ready.

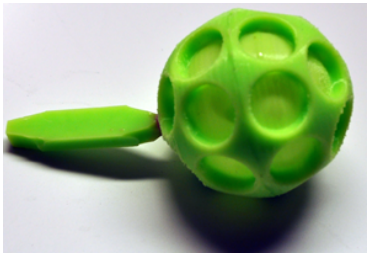

Figure 2.7: The first prototype.

Then came yet another experimental challenge, since I had tremendous difficulties in finding a pump with a controllable flow rate. With the help of a biochemistry lab, I found a pump that I used at its very minimum power. But its vacuum gauge was much too coarse, and had no markings in the range in which I was using it. So I created a water manometer to take my measures, branched on the pipe between the pump and the ball.

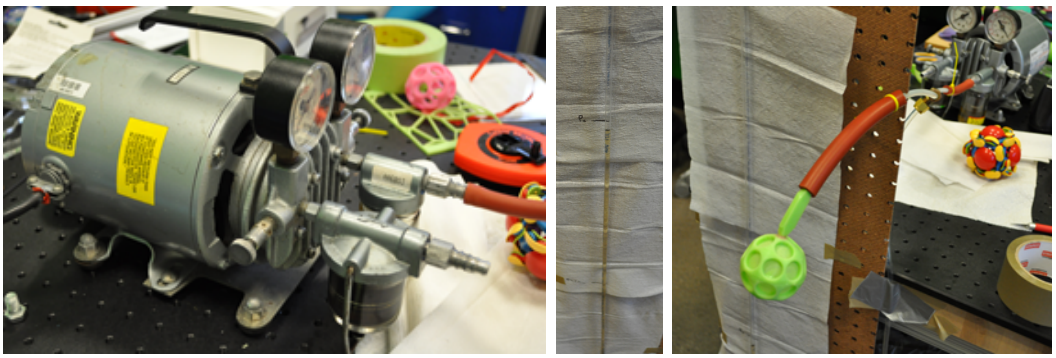

(a) The pump

(b) Water manometer

(c) Ball at the end of the pipe

Figure 2.8: Details of the experimental set-up for pressure controlled experiments.

The result displayed here is a pressure to percentage of the original volume of the ball, following the formula $\frac{V_0 - V}{V_0}$.

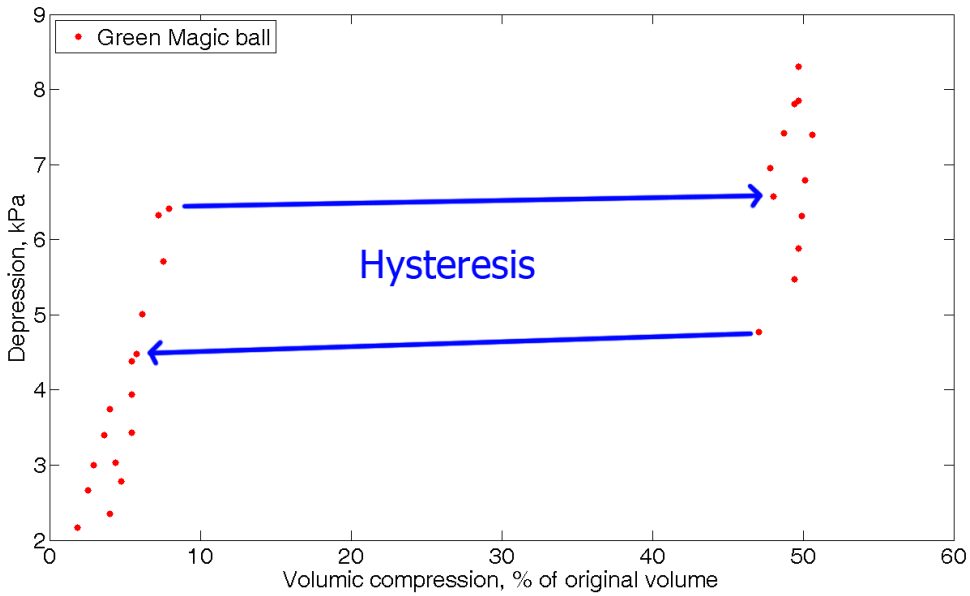

Figure 2.9: Pressure to percentage of original volume.

On this graph we can see two things. First the final volume of the ball is 50% of the starting volume. Second, there is a strong hysteresis and the ball stays folded for a while when the pressure is released.

Conclusion

With a duration of only six months, this internship was very intense, and this report rich in new results. I am aware that what I did on the first project is merely a start, but I am glad that I could discover enough material for a few PhD theses... Regarding the second project I am glad that I could give it a new start, and I am very eager to follow the advancements that will be done.
I have learnt a lot of new things, in a very large span of domains, which made my internship very enjoyable. What I learnt includes many experimental techniques, a lot of theory, using a CAD program and the further practice of two programming languages. I am very happy of the work I have started on both projects, and I do hope that they will keep me busy in the future.

Acknowledgments

I would like to thank warmly Pedro Reis for the opportunity he gave me to spend 6 months in his lab at the MIT. I cannot emphasize enough how happy I was, and still am about the whole internship both from a scientific and from a human perspective. I am also very thankful to Katia Bertoldi, who seemed very happy to have me involved in her research ; I am even happier that I could contribute a little to it.

I would like to also acknowledge Jongmin Shim's hard work and availability. I also thank all the students from civil engineering who have helped me during the internship, especially the "Red Cement" group.

I am grateful to Professor L. Anand, who let me follow his course on Mechanics of solid materials.

Some very special acknowledgments go to Joël Marthelot, Fanny Mas and Jean-Arthur Olive who managed to deal with my various moods and requests during those six months. They also made this internship an unforgettable experience for me. I would like to tell the various people who came to see me in the US that they all helped me in their personnal way, more than they may imagine.

My regard goes to all those involved in what follows : Mountain Dew, roller skating, underground corridors, going back to France on a two days notice, being my roommate, booking the same plane as me, doing an internship in the same town as me, helping me find poutine in Montréal, *not* stealing my bikes, expired bakery, and, most of all, entering random shops in New York.

Bibliography

[1] A. Vaziri and L. Mahadevan, *Localized and extended deformations of elastic shells*, Proceedings of the National Academy of Sciences of the United States of America, 2008, **105**, 23, p. 7913–7918.

[2] B. Audoly and Y. Pomeau, *Elasticity and geometry: from hair curls to the nonlinear response of shells* Oxford University Press, July 2010, Book.

[3] K. Bertoldi, P.M. Reis, S. Willshaw and T. Mullin, *Negative Poisson's ratio behavior induced by an elastic instability*, Advanced Materials, 2009, **21**, 1.

Appendix A

Measuring the Young's modulus of the polymer

The Young's modulus of the polymers I used is a very important piece of information which was not provided by the manufacturer. I had to measure it by myself in a proper way, so that I could normalize my data and collapse my curves. I asked around the department of mechanical engineering, and I was advised to do an extension test on a "dogbone" shape.

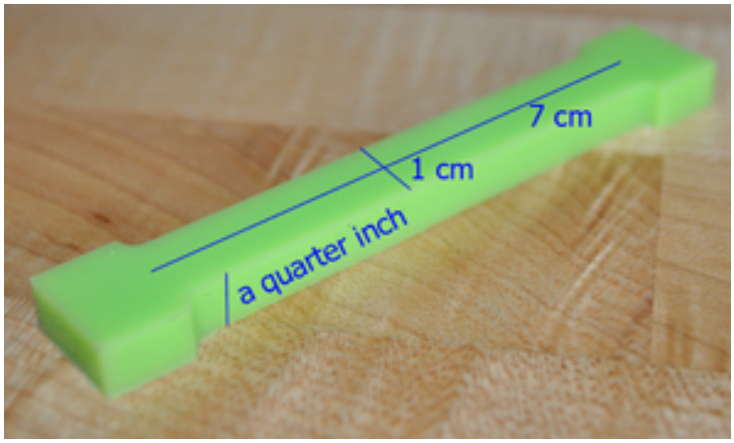

Figure A.1: The shape used for the extension test.

The curves obtained are very linear and since my load cell is very sensitive, I could get very precise values for the Young's modulus :

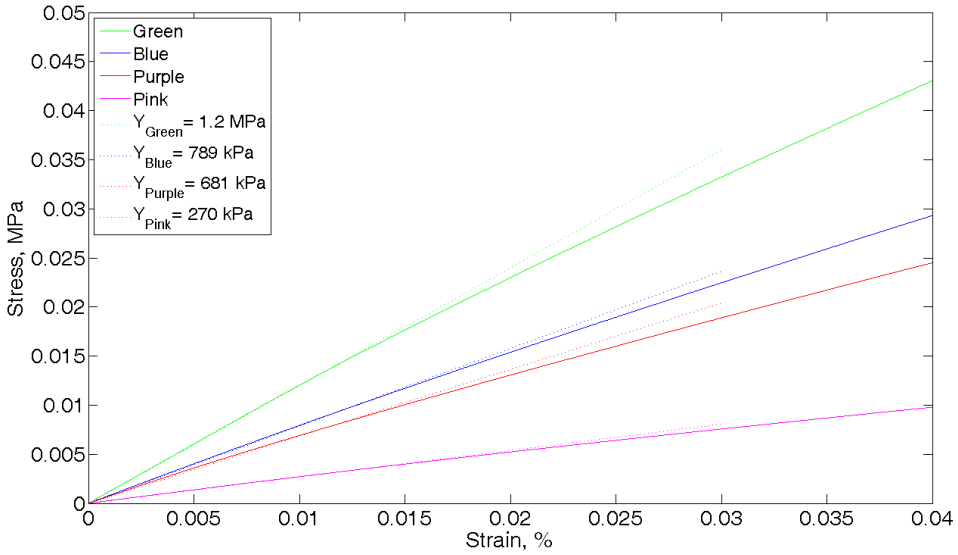

Figure A.2: The linear curves obtained and their fittings.

In the end the Young's moduli measured are :

Polymer color	Green	Blue	Purple	Pink
Young's modulus	1.20 MPa	789 kPa	681 kPa	270 kPa

Appendix B

Additional work on thin shells

What is the ridge height during the compression ?

Under point load, the height of the shell varies. In the case of a simple cap inversion, with every new mm of the screw penetrating the shell, the shell loses .5 mm in height. To convince yourself of this idea, imagine the screw having penetrated the total height of the shell, like on image 1.2(d).

In that situation the shell height is one half of the original height. Hence, we expect the height of the shell to be reduced by one half of the penetration. Here is the measurement result, compared with a perfect one half variation in purple :

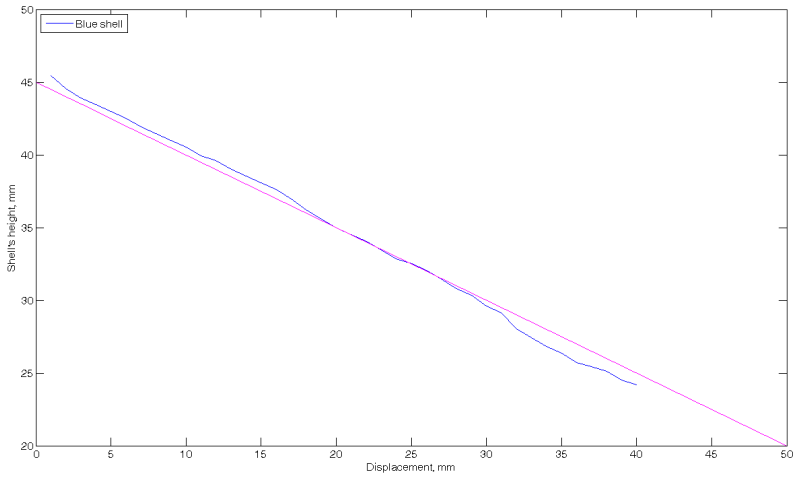

Figure B.1: The linear curves obtained and their fittings.

Does the material used have aging issues ?

The color of the pink shell, for example, changes over time. This means that the polymer ages after a few weeks. But does this aging have an influence on the mechanical properties of the polymer ? The answer is no, as evidenced by this graph, which shows two tests on the same shell separated by 2 months.

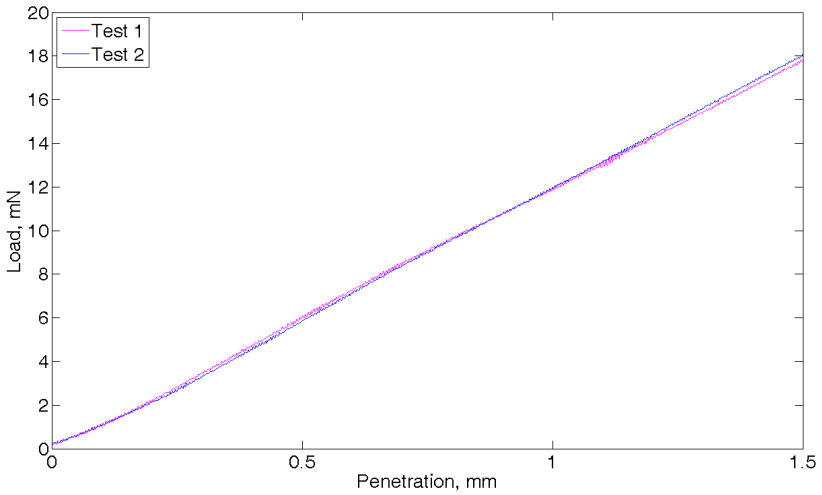

Figure B.2: Two tests on the same shell, separated by two months.

Is the error on the thickness implied by the casting process a real issue ?

The error on the thickness is an issue for us, because the results vary from one shell to the other. But if we cast many shells out of the same mold and then test them, we can pinpoint the error range of our measurements.

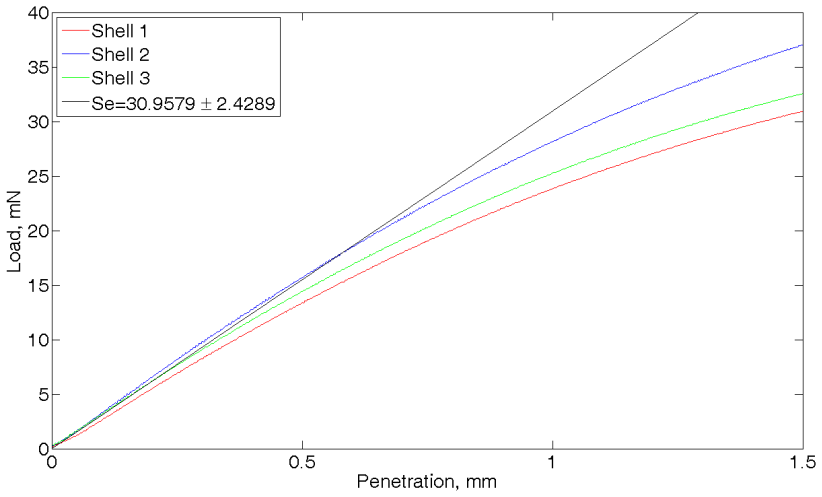

Figure B.3: Three different shells, all casted in the same mold.

The error on the measured Young's modulus is of 8%. This is a reasonable result, and is good to have in mind.

Do the curves I study depend on the position of the screw ?

The answer is, surprisingly enough, no, not at all. When centering the screw under the shell by the eye, an experimental error necessarily occurs. But, doing repeated experiments, and replacing the screw under the shell, I got curves that perfectly overlapped, just as if I had not moved the position of the screw at all !

Is the 3D printing process precise enough to guarantee a precise thickness ?

Unfortunately, the answer was thought to be yes until the very end of my internship. But, when I printed a mold with a ratio $\frac{b}{a}$ of $\frac{3}{2}$ it clearly had a thickness defect : it made the shells casted out of it much stiffer than they should have been. This defect on the mold is visible to the eye, and raises concerns about our ability to study shells when they are thinner than 1 mm...

Under plate loading, is the yield strain dependant on the strain rate ?

The answer to this question seems to be no. The following graph illustrates this statement :

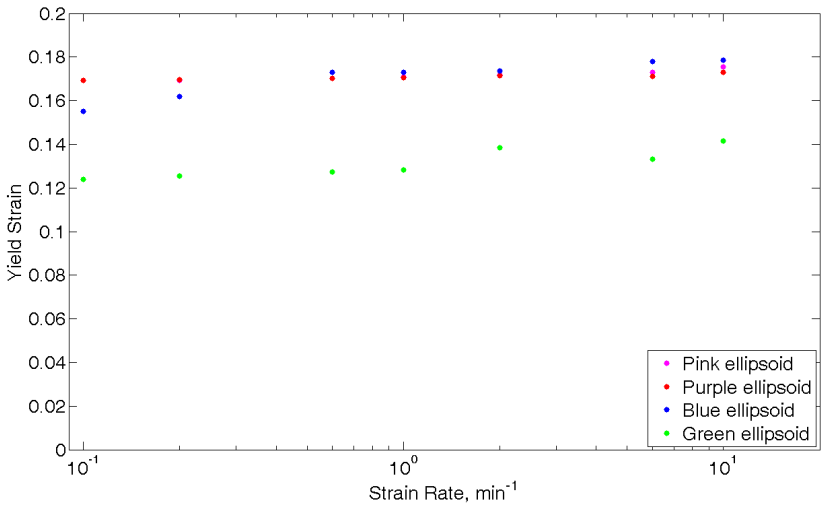

Figure B.4: Yield strain of 1 mm shells against strain rate.

Appendix C

3D Printer : Connex 500

The 3D printer is a commercial machine available at Connex. It enables additive creation of objects of any shapes using a layer by layer procedure.

The machine basically looks like a giant printer, or a photocopier :

Figure C.1: The Connex 500

This machine is very expensive, around 750 k$, and is owned by another MIT laboratory. It is available for usage by any MIT affiliate as a service. The printer can make objects out of a range of plastics with different properties. It is possible to print an object out of two different materials at the same time, so it can have parts of different stiffnesses. Since the printer creates the object layer by layer it should not be possible to have hanging parts, i.e. not laying on a previous layer. That is why the printer also uses a support material, which fills all the holes of the structure. This makes it possible to create any kind of part, even moving or intertwined parts.

The cost of operation of this machine is dreadfully high, which did not make it a possible solution for us on the long term. But for objects of small size the possibilities are infinite and not too expensive. That is why it is used either to complete an experimental set up or to create experimental objects.

Appendix D

The Laser Cutter

This machine uses a laser beam to cut through various materials. It is very simple to use and cuts very quickly. It enables the construction of experimental set-ups and devices in much less time than would be necessary to make them out of metal in a hobby shop. The whole lab uses it extensively to create a variety of objects out of plastic. But the laser cutter can be tweaked so as to cut thin sheets of metal, paper, cardboard etc.

Figure D.1: The Versalaser laser cutter, its air filter and the computer controlling it.

The plastic we used is ABS, and it comes in various thicknesses, usually 1 cm or thinner. It is very easy to cut holes and precise shapes, which makes 3D assemblies easy using a plastic bonder or a couple of screws. The laser cutter follows a vector path (designed in Adobe Illustrator for example), and is recognized by the computer as a printer. Hence once you get the wished design ready, you just have to use the print function of the software.

The laser cutter is able to cut or engrave a material. It also has a raster mode that makes it possible to engrave a grayscale image.

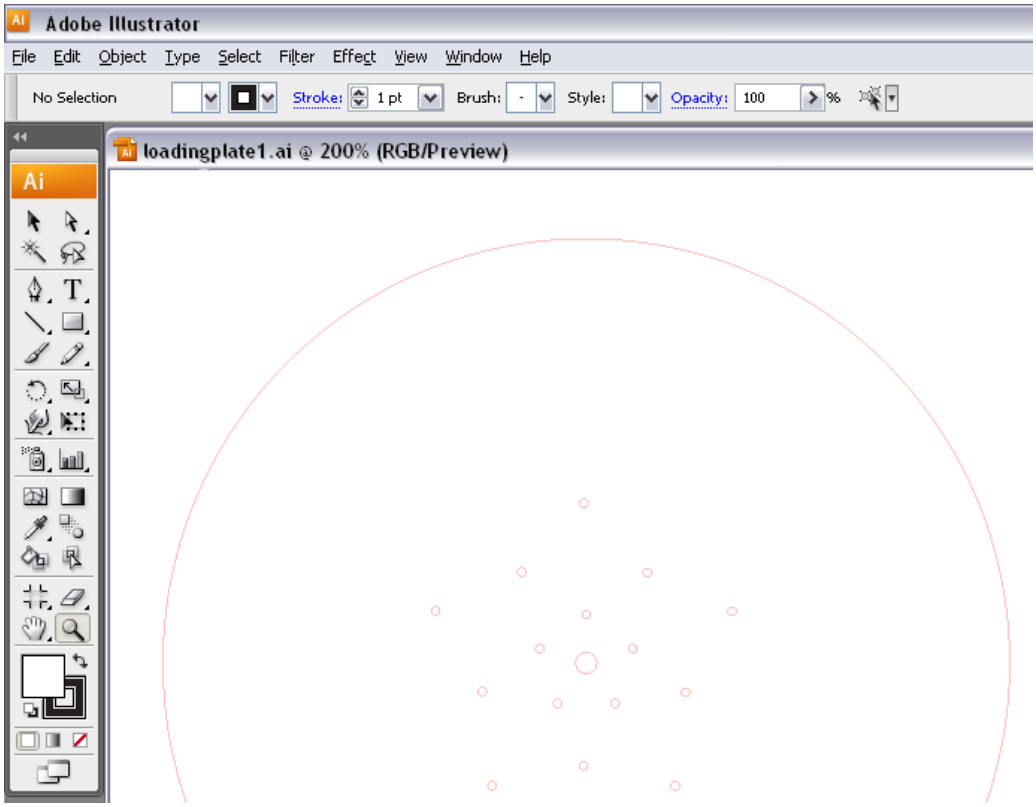

Figure D.2: A vector path for the laser cutter in Illustrator.